

On the statistical mechanics of prion diseases

A. Slepoy, R.R.P. Singh, F. Pázmándi*, R.N. Kulkarni and D.L. Cox

Department of Physics, University of California, Davis, CA 95616

(October 29, 2018)

We simulate a two-dimensional, lattice based, protein-level statistical mechanical model for prion diseases (e.g., Mad Cow disease) with concomitant prion protein misfolding and aggregation. Our simulations lead us to the hypothesis that the observed broad incubation time distribution in epidemiological data reflect fluctuation dominated growth seeded by a few nanometer scale aggregates, while much narrower incubation time distributions for inoculated lab animals arise from statistical self averaging. We model ‘species barriers’ to prion infection and assess a related treatment protocol.

PACS Indices: 82.30.-k, 82.35.Pq, 87.15.Cc

Transmissible neurodegenerative prion diseases, such as Mad-Cow Disease (BSE) and Creutzfeldt-Jakob Disease (CJD) in humans, increasingly represent a serious public health threat [1]. Prusiner and collaborators have shown that the infectious agent (prion) in these diseases consists of a quantity of a misfolded form (PrP^{Sc}) of the ~ 200 amino acid PrP^{C} protein which is expressed ubiquitously in mammalian neurons [2]. The PrP^{C} proteins normally reside on neuron surfaces [4], and the more hydrophobic PrP^{Sc} forms tend to aggregate: large (micron scale) PrP^{Sc} amyloid plaques are a common post-mortem feature of brain tissues, and fibrils are observed in *in vitro* experiments. Nucleic acid free propagation demands that PrP^{Sc} autocatalyze their own formation by helping to convert more PrP^{C} into PrP^{Sc} [2,3]. Given that mammalian PrP^{C} differ by only 5-10% in amino acid composition and that variant CJD correlated with BSE has been observed in England, the efficacy of “species barriers” in limiting transmission is of considerable interest.

Several facts suggest that prion disease may be driven less by complex biology (as in Alzheimers’ disease) than by physico-chemical processes, including: (1) The “universal character” of sporadic CJD, observed globally without evident spatio-temporal clustering at an annual background death rate of 0.5-1.5/million and mean onset age of about 63 years [6]. (2) Highly reproducible incubation time vs. infectious dose distributions observed in laboratory animal studies, with a power law relation between mean incubation time and dose concentration D [7]. (3) The close temporal proximity of disease onset and death. (4) PrP^{Sc} may be grown *in vitro* without biological processing and is toxic to neurons, though not yet demonstrably infectious [5]. The following question is thus raised: *is the incubation time of prion disease dominated by a fundamental physico-chemical nucleation and growth of PrP^{Sc} protein aggregates?*

We present simulation results for a simple two-dimensional, lattice based statistical mechanical model for prion disease based at the protein level. It is all but hopeless to develop an atomic level simulation capable of spanning the 21 temporal orders of magnitude between picosecond scale intra-protein motion and the potentially

decades long incubation times of large prion aggregates. Our simulation is a bridge between the short distance and time scales covered in individual protein models and the long time, macroscopic realm of chemical kinetics. We use our simulations to identify the protectorate of principles necessary to describe the aforementioned universal features of prion disease. Specifically, we find: (1) Concomitant PrP^{Sc} autocatalysis and stable aggregation can explain the long disease incubation times, and the difference between sporadic (unseeded) and infectious (seeded) onset. This principle is consistent with data for yeast prions [10], is closely related to the earlier nucleation theory of Lansbury [8], and avoids the need to fine tune model parameters with separated autocatalysis and aggregation [9]. (2) The distributions of disease incubation times (well defined onset edge, broad fluctuation driven spectrum for dilute prion doses, narrow short time shifted distribution for more concentrated prion doses) strongly suggest a central role for growth from a minimally nanometer scale seed (with order 10 PrP^{Sc} proteins). With these assumptions we obtain a one parameter fit to the BSE incubation time data, an order of magnitude correct estimate of the mean incubation time for BSE and infectious CJD, and we argue that self-averaging explains a narrowing of incubation time distributions observed in the laboratory [7,11]. Finally, by considering both sticking and interconversion rate differences for prions of different species, we provide a theoretical underpinning to data for the species barrier efficacy and to proposed treatments based upon coating of incipient prion plaques.

Our assumption of two-dimensionality is consistent with the observation that PrP^{C} resides on neuron surfaces and autocatalysis and aggregation must certainly initiate there. The lattice structure should be irrelevant at long times. By assuming a triangular lattice we minimize the anisotropy (which appears first in rank six tensors for hexagonal lattices). This simulation yields the crucial qualitative features necessary to specify the “prion protectorate.” Our resulting prion aggregates are essentially amorphous, rather than quasi-one-dimensional filaments as found in some *in vitro* experiments. We shall discuss an anisotropic simulation yielding fibrils elsewhere.

Our model is based upon the energy landscape schematized in Fig. 1. Individual lattice cells take on three values: unoccupied (implicitly filled with water), occupied by a PrP^C protein, or occupied by a PrP^{Sc} protein. At the beginning of each simulation, we choose a monomer PrP^C configuration distributed randomly, with a number (0-4) of PrP^{Sc} seeds located randomly as well.

In the spirit of cellular and molecular automata, we eschew an explicit Hamiltonian based molecular dynamics in favor of the following updating rules, specified in time units of one full lattice sweep (d is the nearest neighbor coordination number):

- (1) Identify each occupied cell as PrP^C or PrP^{Sc} by checking its number of nearest neighbors.
- (2) For each PrP^C, move one step in a random direction if that adjoining site is unoccupied.
- (3) Identify aggregates (size N_P) by PrP^{Sc} presence; move them per Rule (2) with probability $1/\sqrt{N_P}$.
- (4) For $d = 0, 1$ the protein remains PrP^C.
- (5) For $d = 2$, the protein is PrP^C or PrP^{Sc} with equal probability
- (6) For $d \geq 3$ the protein is PrP^{Sc}.

Rules (1-3) ensure diffusive motion of PrP^C monomers and PrP^{Sc} aggregates. Rules (4-6) specify protein interactions and autocatalysis, and reflect the relative hydrophobicity of PrP^{Sc}. To assure the biologically plausible condition of constant average PrP^C concentration, at the start of a new sweep we randomly place a new PrP^C for each lost in the previous update.

This procedure is repeated for up to millions of full sweeps through the lattice. Note that a sweep defines the minimum time scale for conversion of PrP^C to PrP^{Sc}, which is presumably of order a second or less in real time. We work with maximum lattice sizes of $N = 4 \times 10^4$. Practically, we are able to run at areal monomer concentrations $c \geq 0.1\%$, which are likely to be about three orders of magnitude larger than in the brain.

We run our seeded simulations repeatedly following the largest nano-aggregates until they reach a size of up to 0.4% of the lattice. Each seed consists of 10 PrP^{Sc} monomers [12] For a given aggregate size, we have studied the properties of the distribution of lifetimes to reach that size. For a final aggregate size of $\mathcal{A}=0.2\%N$ (80 monomers) we display the corresponding distributions P_D in Fig. 2(a) for several values of c and $D = 1$. P_D displays greater fluctuations for small c , and increasing c shifts P_D to short times. Fluctuations dominate the growth from the small seed aggregate. For larger \mathcal{A} we find that the onset time grows sublinearly in \mathcal{A} , while the distribution width grows weakly with \mathcal{A} . To within fluctuations, the P_D curves for different c collapse when scaled by the mean time t_m . (The curves broaden somewhat for $D = 2, 3, 4$.) This implies the scaling law

$$P_D(t, c) \approx \frac{1}{t_m(c)} F_D\left(\frac{t}{t_m(c)}\right) \quad (1)$$

In the range of concentrations studied, we can fit $t_m(c)$ well by either: (a) the polynomial form $t_m(c) \sim Ac^{-1} + Bc^{-2}$ (the first term reflecting monomer aggregation, the second representing dimer aggregation), or (b) a power law form, $t_m(c) \sim c^{-\alpha(D)}$, with $\alpha(D) = 1.66(D = 1)$, $1.49(D = 2)$. For finite \mathcal{A} and $c \rightarrow 0$ the exponent $\alpha(D)$ should tend to two, reflecting dominant dimer aggregation. Fit (b) is consistent with a nontrivial scaling limit as $\mathcal{A} \rightarrow \infty$, $c \rightarrow 0$. Both fits to $t_m(c)$ give order of magnitude equivalent extrapolations to lower c relevant to biological contexts. Assuming $t_m(c) \sim D^{-\beta}$ at fixed c , we estimate $\beta \leq 1$ with large numerical uncertainty. Taken together, these data lead us to a conjecture of *asymptotic compression* of P_D : for $c \rightarrow 0$, an increasingly large range of \mathcal{A} will have essentially the same scaled shape, because the time t_2 it takes to go from \mathcal{A} to say, $2\mathcal{A}$ will be much smaller than t_m for going from $10 \rightarrow \mathcal{A}$.

We believe that other processes, such as protease attack or competition between PrP^{Sc}-PrP^{Sc} and PrP^{Sc}-neuron binding will limit prion aggregation on the neural surface and cause fissioning and spreading of nano-aggregates to other neurons. Such fission is necessary for exponential growth of infectious agents, as noted previously [14]. At the order-of-magnitude level t_2 sets the doubling time for disease spread, assuming that inter-cellular diffusion rates exceed intra-cellular ones. Given $t_2 \ll t_m$ (at biological c values) both in our fission hypothesis and experiment, slow growth fluctuations for small seed aggregates can dominate the overall incubation time for disease. For example, in hamster experiments the first observable levels of PrP^{Sc} in brain tissues occur at about 90 days, with symptom onset at 120 days, and a doubling time of 2 days [13]. Given the conjectured asymptotic compression, the incubation time distribution will be relatively insensitive to a wide range of nano-aggregate sizes for fission parents or progeny.

We stress several points of agreement with observation and laboratory data. First, we always find death (runaway growth of a killer aggregate) in the presence of infection, in agreement with experiment and the aggregate nucleation hypothesis for prion disease. Second, our rough scaling of t_m with D agrees qualitatively with the extraordinarily reproducible dose vs. incubation time data of Prusiner and collaborators for prion infection in laboratory mice, for which $\tau_I \sim D^{-.62}$. Third, our lifetimes are in order of magnitude agreement with observed BSE incubation times and new variant CJD death ages, which we can prove by exploiting our concentration scaling. For a single seed, at our lowest concentration of 0.1% our distribution peaks at about 10^4 sweeps. Assuming a literature estimate of concentration of *in vivo* prions in solution of 100 nanomole/liter [15] and a protein diame-

ter of order one nanometer suggests a dimensionless areal concentration of about $10^{-3}\%$. With the above concentration scaling this gives an incubation time of about 10^8 sweeps. If we take the 5 year mean incubation time for BSE this implies our basic misfolding time (one sweep) is about one second, which is reasonable at the order of magnitude level. Finally, by simply scaling time for $\mathcal{A} = 80$ by the mean time t_m , we achieve an exceptionally good fit (\mathcal{A}) of the inferred incubation time distribution for BSE in the United Kingdom (for cattle born in 1987) [16] to our scaling curve as shown in Fig. 2(b). This supports our hypothesis that runaway autocatalytic aggregation seeded by a few prion nano-aggregates triggers the disease. This is very plausible since (i) infection is believed to have come from rendering plant offal derived from many animals after considerable processing, leading to substantial dilution, and (ii) prion transmission by oral consumption is estimated to be less efficient than inoculation by a factor of 10^9 .

Sporadic CJD develops in the absence of any infection or genetic predisposition to prion disease. We have studied the lifetime distributions in this case and find that they are very different in shape than the seeded runs, being much broader and dimer fluctuation dominated (peaks scale as c^{-2}). For our estimated biological concentration of $c = 10^{-3}\%$, this could give a mean onset time as large as 10^3 years. Assuming a constant height tail from the minimum single seed onset to the mean human lifespan taken with the 1 part in 10^6 odds of dying from sporadic CJD gives an estimate of a total death probability of a part in 10^5 up to this mean on-set time. This is consistent with our simulations, but not resolvable currently.

In contrast to the breadth of our single seed lifetime distributions, in the event of dosing by a greater number of seeds, self-averaging will narrow the distribution, collapsing it towards the onset (shorter times). Assuming growth proceeds independently for different seeds (which is quite reasonable for the low concentrations in living organisms) distributions would narrow by \sqrt{D} . Several *in vivo* experiments show distribution time narrowing with increased dosage, but are not amenable to quantitative analysis at this time [7,11].

We turn now to the species barrier. To simulate interspecies transmission we replace the integer-valued coordination, the key parameter which determined the stability of different protein conformations in the earlier studies, by a new variable $x = N + N' \times P$ for PrP^C and $x' = N' + N \times P'$, for $\text{PrP}^{C'}$, where N is the number of $\text{PrP}^{C,Sc}$ neighbors and N' the number of $\text{PrP}^{C',Sc'}$ neighbors. The parameters P and P' (chosen less than unity) provide a measure of the reduced effectiveness of interspecies conversion. To deal with the continuous variable x , rather than the integer coordination used earlier, we represent the PrP^C to PrP^{Sc} conversion probability $f(x)$ by

$$f(x) = \frac{1}{e^{\beta(x-2)} + 1} \quad (2)$$

with a similar definition for $\text{PrP}^{C'} \rightarrow \text{PrP}^{Sc'}$ conversion. A separate parameter describes physisorption to an aggregate of alien prions. We allow a $\text{PrP}^{C,Sc}$ cluster of mass M ($M = 1$ being a monomer) to desorb from an alien prion aggregate with probability q^K/\sqrt{M} , where q is the physisorption parameter, and K is the number of units in the cluster adjacent to the alien aggregate. We define q' for $\text{PrP}^{C',Sc'}$ similarly. Thus, we describe species barriers in terms of the two parameters affecting conversion rates (P, P') and physisorption (q, q'). Making $P \neq P'$ and $q \neq q'$ allows for an asymmetry in infectivity, and we can model one of the most striking aspects of the species barrier, namely its asymmetry (*e.g.* mice infect hamsters well, hamsters infect mice poorly).

We have carried out several simulations relevant to the species barrier. First, we have placed alien prion ‘walls’ on a boundary, representing a single large aggregate from another species. With suitable choice of parameters, this leads to the asymmetric species barrier between two species. Namely, disease onset in one species (with large aggregates) and only sub-critical PrP^{Sc} concentration near the wall in the other. Recent experimental data has also shown the build up of such sub-critical PrP^{Sc} concentration in the asymmetric interspecies transmission [17].

Second, suppose the asymmetry is such that $P \ll P'$. In this case, $\text{PrP}^{Sc'}$ is more favorably formed from $\text{PrP}^{C'}$ in the presence of a seed aggregate of PrP^{Sc} than PrP^{Sc} is formed from PrP^C in the presence of a $\text{PrP}^{Sc'}$ seed. Thus, by injecting a large enough initial dose of alien $\text{PrP}^{C'}$ proteins into the organism, it should be possible for $\text{PrP}^{C'}$ to compete favorably with PrP^C for aggregation, and thus extend the incubation time. Such protocols have been tested experimentally: (i) Experiments with the coating dye molecule Congo Red [18] reveal a surprising *non-monotonic* dose vs. lifetime relation: small Congo Red concentrations yield a reduced time for incubation, while larger Congo red concentrations significantly extend the incubation time. (ii) *In vitro* experiments show that the above coating scenario with alien prions works [19] when the initial $\text{PrP}^{C'}$ concentration $c' > c$.

We find both of these experimental features in our simulation as shown in Fig. 3. For $c'/c < 2$, the incubation time is slightly shortened, while for $c'/c > 2$ the incubation time is increased. We find that the lifetime shortening arises because once a few $\text{PrP}^{C'}$ aggregate, they partially block the motion of adjacent PrP^C proteins, enhancing the misfolding probability of the latter. However, further PrP^C misfolding is significantly reduced once $\text{PrP}^{Sc'}$ coats the seed.

A crucial test of our theory would be to monitor, *in vitro*, the lifetime distributions of normal prion proteins

seeded by small aggregates as a function of both c and D to look for the scaling behavior. If it is not possible to easily achieve $D = 1, 2$, presumably the distribution of Fig. 2(b) could be estimated by extrapolation from successively diluted PrP^{Sc} doses. This would also test the extent to which the self-averaging applies. If our single seed hypothesis is correct, it is important to assess how passage occurs upon infection.

Theoretically, it is important to extend our model by including internal degrees of freedom for the proteins which can provide an orientational dependence to the aggregation, allowing for linear fibril formation as opposed to amorphous aggregates. This connects naturally with simulations on individual proteins, and also allows for the study of different protectorates for collective protein phenomena.

Acknowledgements. We acknowledge useful discussions with S. Carter, F. DeArmond, R. Fairclough, C. Ionescu-Zanetti, T. Jue, R. Khurana, and C. Lasmézas. F. Pázmándi has been supported by National Science Foundation Grant DMR-9985978. R.R.P.S. and D.L.C. have benefitted from discussions at workshops of the Institute for Complex Adaptive Matter. We are grateful for a grant of supercomputer time from the Lawrence Livermore National Laboratory.

* Also at: Theoretical Physics Department, University of Debrecen, P.O. Box 5, H-4010 Debrecen, Hungary, and Research Group of the Hungarian Academy of Sciences, Institute of Physics, TU Budapest, H-1521 Hungary.

- [1] See for example, A. Coghlan, *New Scientist* **168**, 4 (2000).
- [2] S.B. Prusiner, in **Prion Biology and Diseases**, ed. S.B. Prusiner (Cold Spring Harbor Laboratory Press, Cold Spring Harbor NY, 1999), p. 1.
- [3] J.S. Griffith, *Nature* **215**, 1043 (1967).
- [4] S.B. Prusiner *et al.*, ref. 2 *op. cit.*, p. 349.
- [5] K. Post *et al.*, *Arch. Virol.* (Supp. **16**), 265 (2000).
- [6] R.G. Will *et al.*, ref. 2 *op. cit.*, p. 465.
- [7] S.B. Prusiner *et al.*, ref. 2 *op. cit.*, p. 113.
- [8] J.H. Comb, P.E. Fraser, and P.T. Lansbury Jr., *Proc. Natl. Acad. Sci. (USA)* **90**, 5959 (1993).
- [9] M. Eigen, *Biophys. Chem.* **63**, A1 (1996).
- [10] T.R. Serio *et al.*, *Science* **289**, 1317 (2000).
- [11] C.I. Lasmézas *et al.*, *Science* **275**, 402 (1997).
- [12] The minimally stable seed in our model has seven monomers, but exhibits spurious barriers for transitioning from seven to ten monomers.
- [13] M. Beekes, E. Baldauf, and H. Diringer, *J. Gen. Vir.* **77**, 1925 (1996).
- [14] J. Masel, V.A.A. Jansen, and M.A. Nowak, *Biophys. Chem.* **77**, 139 (1999).
- [15] M. Laurent, *FEBS Lett.* **407**, 1 (1997).

- [16] R.M. Anderson *et al.*, *Nature* **382**, 779 (1996).
- [17] A.F. Hill *et al.*, *Proc. Nat. Acad. USA* **97**, 10248 (2000).
- [18] H. Rudyk *et al.*, *J. General Virology* **81**, 1155 (2000).
- [19] M. Horiuchi *et al.*, *Proc. Natl. Acad. Sci. (USA)* **97**, 5836 (2000).

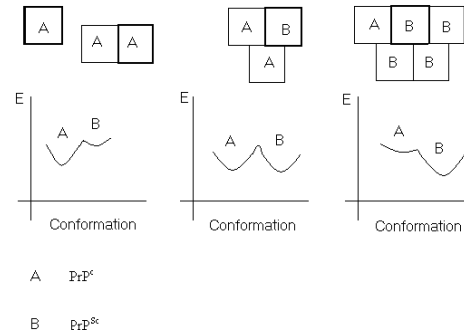


FIG. 1. Schematic energy landscapes for model prion proteins. Upper figures show proteins in varying coordination environments corresponding to rules (1-6), lower figures show schematic energy landscapes.

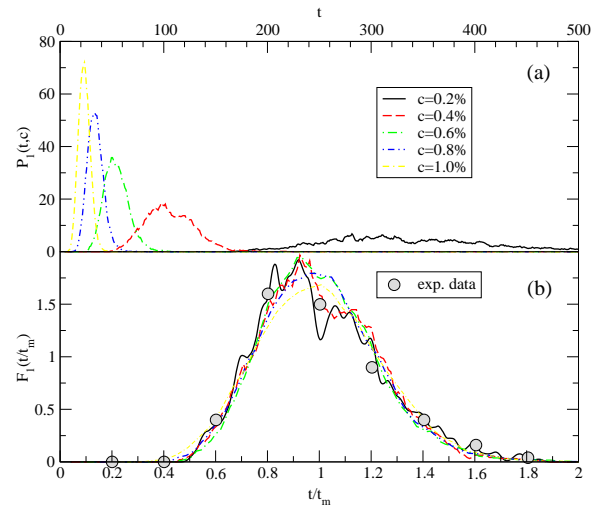


FIG. 2. Aggregation lifetime distributions $P_D(t, c)$ for a single seed ($D=1$). Seeds have ten proteins, simulations terminate at aggregate size $\mathcal{A} = 80$, time is measured in units of 10^4 full lattice sweeps. (a) Dependence upon areal concentration c of normal prion proteins. (b) Scaled distribution $F_1(t/t_m)$ vs. t/t_m . t_m is the mean lifetime for a given concentration. Points are inferred incubation time data for BSE-infected cattle in the United Kingdom born in 1987.

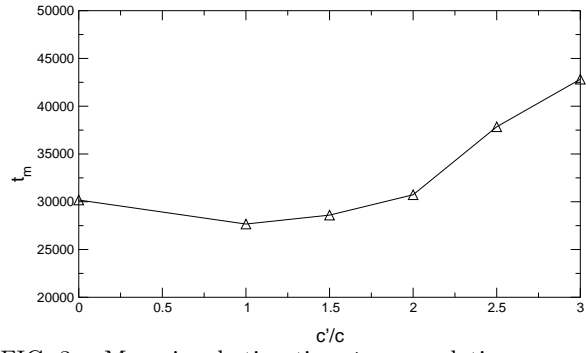


FIG. 3. Mean incubation time t_m vs. relative concentration of alien prions c'/c (test of coating treatment; see text for discussion).